

Received September 16, 2021, accepted October 6, 2021, date of publication October 8, 2021, date of current version October 15, 2021.

Digital Object Identifier 10.1109/ACCESS.2021.3118899

A Multiple-Jammer Deceptive Jamming Method Based on Particle Swarm Optimization Against Three-Channel SAR GMTI

XIN CHANG¹, YANBIN LI¹, YAN ZHAO^{1,2,3}, AND YUFENG DU^{1,2}

¹The 54th Research Institute of China Electronics Technology Group Corporation (CETC54), Shijiazhuang 050081, China

²Hebei Key Laboratory of Electromagnetic Spectrum Cognition and Control, Shijiazhuang 050081, China

³National Laboratory of Radar Signal Processing, Xidian University, Xi'an 710071, China

Corresponding author: Xin Chang (changxinydb@163.com)

This work was supported by the China Postdoctoral Science Foundation under Grant 2021M693002.

ABSTRACT Traditional deceptive jamming methods effectively generate false targets against three-channel synthetic aperture radar ground moving target indication (SAR GMTI). However, effectiveness of traditional methods is limited to azimuth distance between two jammers. When the distance requirement is not satisfied, the jamming amplitude coefficients will be too high to be used by jammers. To overcome this disadvantage, a novel multiple-jammer deceptive jamming method is proposed. The intercepted radar signal is retransmitted and performed by amplitude and time-delay modulation. Then, jamming signal is first modeled as a polynomial function where the polynomial order is equal to the number of jammers. The interferometric phase difference between a moving target and a false target is utilized as an objective function, the azimuth relocated position difference between a moving target and a false target is utilized as the constraint to reduce computational burden, and the optimal jamming amplitude coefficients are estimated by solving the optimization problem based on the particle swarm optimization (PSO). Hereby, the optimal jamming amplitude coefficients and gain calculated with the proposed method will be lower than those calculated with traditional methods when the distance requirement is not satisfied. By utilizing the optimal coefficients and jamming amplitude gain, a false target generated with the proposed method will be detected by displaced phase center antenna (DPCA) technique and be relocated in the desired position by along-track interferometry (ATI) technique. Experimental results verify the effectiveness of the proposed method.

INDEX TERMS Synthetic aperture radar (SAR), ground moving target indication (GMTI), displaced phase center antenna (DPCA), along-track interferometry (ATI), deceptive jamming, particle swarm optimization (PSO).


I. INTRODUCTION

Synthetic aperture radar ground moving target indication (SAR GMTI) has been widely utilized in both civil and military applications ranged from a city traffic monitoring to an airport surface surveillance and a battleground surveillance [1]–[5]. SAR GMTI is able to detect information of moving targets from sensitive areas. Displaced phase center antenna (DPCA) technique and along-track interferometry (ATI) technique are two important techniques of three-channel SAR GMTI. DPCA technique detects slow moving targets from strong clutter by subtracting two coregistered SAR images, and ATI technique estimates initial

azimuth positions of moving targets by exploiting interferometric phase between two coregistered SAR images [3], [6]–[8]. To prevent moving targets from being detected and relocated by DPCA technique and ATI technique, research on jamming methods against SAR GMTI has been an important subject in electronic countermeasure (ECM).

In general, jamming methods are classified as barrage noise jamming methods and deceptive jamming methods [9]. However, to be against DPCA technique and ATI technique, jamming methods are classified into multiple-jammer jamming methods and single-jammer jamming methods according to the number of jammers.

Single-jammer jamming methods are proposed to enlarge jamming area, reduce computational burden, enhance focus capability, fortify electromagnetic fidelity and raise

The associate editor coordinating the review of this manuscript and approving it for publication was Gerardo Di Martino .

correlation coefficient [10]–[17]. These goals may conflict. For example, a deceptive jamming method with high electromagnetic fidelity may require too many modulations, and radar parameters are obtained by jammers with high accuracy which increases computational burden. Tradeoffs between fidelity and computational burden, between jamming area and focus capability, and so on, are issues in ECM.

However, single-jammer jamming methods are difficult to prevent DPCA technique and ATI technique from detecting and relocating ground moving targets. There are two obvious disadvantages. First, with DPCA technique, an azimuth jamming filter is generated based on the additional phase terms of jamming signal in different channels, and then jamming effect will be suppressed by the filter [18]. Second, all false targets will have the same azimuth relocated position which cannot be controlled with single-jammer jamming methods. Then they will be recognized and cannot mislead radar decision-making [19]. The jamming effectiveness will be significantly reduced. To address these weaknesses, the single jammer is set on an unmanned aerial vehicle (UAV). By controlling velocity of jammer and the position of jammer beam ‘footprint’ which is an area illuminated by the jammer beam, the intercepted radar signal scattered by scatterers performs jamming signal which is the same as the echo of the real moving target. However, jammer power is limited to the scattering coefficient of scatterers [20].

To overcome these disadvantages, multiple-jammer jamming methods are proposed. The barrage noise jamming method based on double jammers is an effective jamming method [18]. Noise covers the whole detection result with DPCA technique, and then the protected target cannot be relocated with ATI technique. Because the noise-like signal cannot obtain SAR processing gain, this method requires high transmitting power. To reduce jamming power, jamming signal should be coherent in range and azimuth to obtain the SAR processing gain, and then the multiple-jammer deceptive jamming methods are proposed to control initial azimuth positions of false targets. By setting jamming complex coefficient for every jammer, the intercepted radar signal is performed by the phase modulation and the time-delay modulation to generate jamming signal, which is similar to the echo of a moving target in every channel. Then, the detection results of a false target will be equal to those of a real moving target with DPCA technique and ATI technique, including the range position, the azimuth position, the impulse response width (IRW), the peak sidelobe ratio (PSLR) and correlation coefficient.

An important problem faced by jammers is how to solve jamming complex coefficients. Considering the complex jamming coefficients can be separated into the jamming amplitude coefficients and the jamming phase coefficients, the method proposed by Zhang *et al.* turns the two-dimension search problem into two simple one-dimension search problems [21], [22]. However, the method need to analyze the monotonicity of the interferometric phase expression varying with amplitude coefficients and the jamming phase

coefficients. It makes the processing of solution too complex and trivial. Sun *et al.* directly makes the sum of the intercepted and modulated signal equal to that of the echo of the real moving target in every channel. Hence, the jamming complex coefficients will be solved by a matrix solution [23]. iChang *et al.* proves that the jamming amplitude coefficients can precisely control azimuth relocated positions of false targets without the jamming phase coefficients, which can reduce the computational complexity. The jamming amplitude coefficients can be directly obtained by solving a quadratic equation with one unknown [24]. Although traditional methods are able to solve jamming coefficients, there is a disadvantage in these methods. The jamming coefficients are solved as a unique solution, and the distance between jammers must be satisfied. When the distance required by traditional methods is not satisfied, the jamming amplitude coefficients could be too high to be used by jammers. Thus, an important problem faced by jammers are that the limitation of the azimuth distance between jammers should be removed, which will lead to reduce the jamming amplitude coefficients.

To overcome this disadvantage, a multiple-jammer deceptive jamming method based on particle swarm optimization (PSO) is proposed against three-channel SAR GMTI. Compared with previous works, the contribution of this paper is that a novel jamming problem modeling idea is proposed based on an optimization problem. By establishing a jamming geometry, the interferometric phase difference between a moving target and a false target is utilized as an objective function, the azimuth relocated position difference between a moving target and a false target is utilized as the constraint to reduce computational burden, and the optimal jamming amplitude coefficients are estimated by solving the optimization problem based on the particle swarm optimization (PSO). After multiple episodes which satisfy decision-making time, coefficients are grouped into the candidate coefficients set. Then the optimal coefficients, which are the lowest coefficients, will be chosen from the candidate coefficients set.

The reminder of this paper is organized as follows. Section II introduces a jamming geometry of the multiple-jammer deceptive jamming method against three-channel SAR GMTI. The detection result of a moving target is derived. Moreover, a multiple-jammer deceptive jamming method is presented. In addition, an important problem about how to solve jamming complex coefficients is analyzed, and a multiple-jammer deceptive jamming method is proposed based on PSO in Section III. The experimental results are given in Section IV. Finally, conclusions are drawn in Section V.

II. A MULTIPLE-JAMMER DECEPTIVE JAMMING METHOD AGAINST THREE-CHANNEL SAR GMTI

In this section, a jamming geometry of a multiple-jammer deceptive jamming method is first presented. Then, the deceptive jamming method is described in detail by analyzing the detection results of DPCA technique and ATI technique.

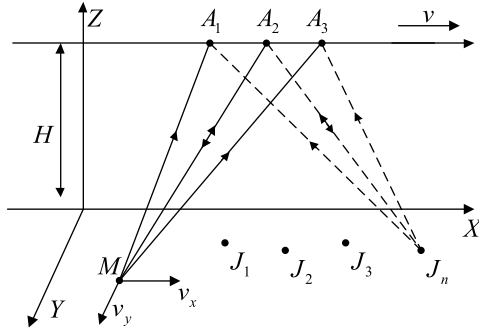


FIGURE 1. Jamming geometry.

A. JAMMING GEOMETRY OF A MULTIPLE-JAMMER DECEPTIVE JAMMING METHOD AGAINST THREE-CHANNEL SAR GMTI

Because radar is a non-cooperative objective, it is hard to obtain the accurate 2-D impulse response of a moving target. Therefore, a jamming geometry is established, and then the algorithm process and the technique used by radar are analyzed based on intelligence support [25]. In addition, with the help of the real-time parameter measurement, the 2-D impulse response of a moving target could be estimated [15], [23]. If the jamming geometry is similar to the real jamming geometry, the verisimilar 2-D impulse response of a moving target will be obtained.

As shown in Fig. 1, a radar works at the board-side mode. It flies at a constant velocity v along with X-axis. X-axis represents the azimuth direction at altitude H , Y-axis represents the ground range direction, and Z-axis represents altitude direction. The three antenna are denoted by the points A_1 , A_2 , and A_3 . Their coordinates are $(vt_a - D, 0, H)$, $(vt_a, 0, H)$ and $(vt_a + D, 0, H)$ varying with t_a where t_a is the slow time and D is the distance among antenna. Especially, jammers can only rely on intelligence support to acquire distance D [25]. The signal is transmitted from antenna A_2 , and then echo is received by antenna A_1 and A_3 . A moving target is denoted by the point M , and its coordinate is $(x_m + v_x t_a, y_m + v_y t_a, 0)$. Assume that the number of stationary jammers is N . The n th jammer is denoted by the point J_n and its coordinate is (x_n, y_n, h_n) , where n is an integer and it serves as the index for each jammer. They modulate the intercepted signal to generate a verisimilar false moving target F , which is similar to the moving target M in the detection result with DPCA technique and ATI technique.

B. THE DETECTION RESULT OF THE MOVING TARGET

The linear frequency modulation (LFM) signal used by the radar can be expressed as follows:

$$S_0(t_r, t_a) = a_r(t_r) \exp \left\{ j2\pi \left[f_0(t_r + t_a) + \frac{\gamma t_r^2}{2} \right] \right\} \quad (1)$$

where t_r is the fast time, f_0 is the radar center frequency, γ is the chirp rate, $a_r(t_r) = \begin{cases} 1 & |t_r| \leq T_r/2 \\ 0 & |t_r| > T_r/2 \end{cases}$ is the pulse envelope of the signal, and T_r is the pulse duration.

A symbol like $R_{MA_1}(t_a)$ is defined as the distance between M and A_1 varying with t_a . It is used to explain the different paths. The slant range of moving target M varying with t_a for antenna A_1 , A_2 and A_3 are respectively expressed as follows:

$$R_{M_1}(t_a) = R_{MA_2}(t_a) + R_{MA_1}(t_a) \quad (2)$$

$$R_{M_2}(t_a) = 2R_{MA_2}(t_a) \quad (3)$$

$$R_{M_3}(t_a) = R_{MA_2}(t_a) + R_{MA_3}(t_a) \quad (4)$$

Considering $v_x \ll v$, $v_y \ll v$ and $D \ll R_M$, the Taylor series expansions of $R_{MA_1}(t_a)$, $R_{MA_2}(t_a)$ and $R_{MA_3}(t_a)$ are respectively expressed as follows:

$$\begin{aligned} R_{MA_2}(t_a) &= \sqrt{(x_m + v_x t_a - vt_a)^2 + (y_m + v_y t_a)^2 + H^2} \\ &= R_M + \frac{[y_m v_y + (v_x - v)x_m]}{R_M} t_a \\ &\quad + \frac{[(v - v_x)^2 + v_y^2]}{2R_M} t_a^2 \end{aligned} \quad (5)$$

$$\begin{aligned} R_{MA_1}(t_a) &= \sqrt{[x_m + (v_x - v)t_a + D]^2 + (y_m + v_y t_a)^2 + H^2} \\ &= R_{MA_2}(t_a) + \frac{x_m D - v D t_a + D^2}{R_M} \end{aligned} \quad (6)$$

$$\begin{aligned} R_{MA_3}(t_a) &= \sqrt{[x_m + (v_x - v)t_a - D]^2 + (y_m + v_y t_a)^2 + H^2} \\ &= R_{MA_2}(t_a) - \frac{x_m D - v D t_a - D^2}{R_M} \end{aligned} \quad (7)$$

where $R_M = \sqrt{x_m^2 + y_m^2 + H^2}$.

In SAR images, the azimuth position of the moving target M is determined by the Doppler frequency at $t_a = 0$ [11]. Then, the azimuth position of the moving target M is described as follows:

$$x'_m = -\frac{R_M}{2v} \left. \frac{d2R_{MA_2}(t_a)}{dt_a} \right|_{t_a=0} = -\frac{[(v_x - v)x_m + v_y y_m]}{v} \quad (8)$$

The baseband echo from a moving target M to antenna A_1 and A_3 are respectively expressed as follows:

$$\begin{aligned} S_{M_1}(t_r, t_a) &= \sigma_M a_r \left[t_r - \frac{R_{M_1}(t_a)}{c} \right] a_{az} \left(t_a - \frac{x'_m}{v} \right) \\ &\quad \times \exp \left[j\pi \gamma \left(t_r - \frac{R_{M_1}(t_a)}{c} \right)^2 \right] \\ &\quad \times \exp \left[-j \frac{2\pi}{\lambda} R_{M_1}(t_a) \right] \end{aligned} \quad (9)$$

$$\begin{aligned} S_{M_3}(t_r, t_a) &= \sigma_M a_r \left[t_r - \frac{R_{M_3}(t_a)}{c} \right] a_{az} \left(t_a - \frac{x'_m}{v} \right) \\ &\quad \times \exp \left[j\pi \gamma \left(t_r - \frac{R_{M_3}(t_a)}{c} \right)^2 \right] \\ &\quad \times \exp \left[-j \frac{2\pi}{\lambda} R_{M_3}(t_a) \right] \end{aligned} \quad (10)$$

where λ is the wavelength of the LFM signal, σ_M is the scattering coefficient of the moving target M , $a_{az}(t_a) = \begin{cases} 1 & |t_a| \leq T_a/2 \\ 0 & |t_a| > T_a/2 \end{cases}$ is the azimuth envelope, and T_a is the target exposure time.

After SAR processing, the SAR images of antenna A_1 and A_3 are expressed as follows:

$$I_{M_1} \left(t_r, t_a + \frac{D}{v} \right) = I_M(t_r, t_a) \exp \left[\frac{j4\pi D}{\lambda R_M} \left(x'_m - \frac{x_m}{2} \right) \right] \quad (11)$$

$$I_{M_3}(t_r, t_a) = I_M(t_r, t_a) \exp \left(\frac{j4\pi D x_m}{\lambda R_M 2} \right) \quad (12)$$

$$I_M(t_r, t_a) = \sigma_M \left(1 - \frac{|t_a - x'_m/v|}{T_a} \right) \left(1 - \frac{|t_r - R_M/c|}{T_r} \right) \times \text{sinc} \left[\pi B_a \left(t_a - \frac{x'_m}{v} \right) \left(1 - \frac{|t_a - x'_m/v|}{T_a} \right) \right] \times \text{sinc} \left[\pi B_r(t_r - t_m) \left(1 - \frac{|t_r - R_M/c|}{T_r} \right) \right] \quad (13)$$

where B_a is the Doppler bandwidth and B_r is bandwidth of LFM.

Based on the DPCA technique, the difference between the two adjacent coregistered SAR images will be expressed as follows [6], [19]:

$$I_{DPCA}^M = \left| I_{M_1} \left(t_r, t_a + \frac{D}{v} \right) - I_{M_3}(t_r, t_a) \right| = 2 |I_M(t_r, t_a)| \cdot \left| \sin \left[\frac{2\pi D(x'_m - x_m)}{\lambda R_M} \right] \right| \quad (14)$$

Based on the ATI technique, the interferometric phase of the moving target M will be described as follows [6], [19]:

$$\hat{\phi}_M = \arg \left[I_{M_3}(t_r, t_a) \cdot I_{M_1}^* \left(t_r, t_a + \frac{D}{v} \right) \right] = \frac{4\pi D(x'_m - x_m)}{\lambda R_M} \quad (15)$$

where $\arg[\cdot]$ represents the operation of extracting phase term and the superscript $*$ represents the complex conjugate. The parameters, D , λ and R_M , belong to radar, and x'_m is the azimuth position of the target in SAR images. Thus, according to (8) and (15), the moving target M will be relocated as follows:

$$\hat{x} = x'_m - \frac{\lambda R_M}{4\pi D} \hat{\phi}_M = x_m \quad (16)$$

Then the detection processing of radar is presented in detail, and the key idea of the proposed method is to simulate detection result of the moving target M by jammers.

C. THE MULTIPLE-JAMMER DECEPTIVE JAMMING METHOD

The slant range of the n th jammer varying with t_a for antenna A_1 , A_2 and A_3 are respectively expressed as follows:

$$R_{F_1}^n(t_a) = R_{J_n A_2}(t_a) + R_{J_n A_1}(t_a) \quad (17)$$

$$R_{F_2}^n(t_a) = 2R_{J_n A_2}(t_a) \quad (18)$$

$$R_{F_3}^n(t_a) = R_{J_n A_2}(t_a) + R_{J_n A_3}(t_a) \quad (19)$$

Taylor series expansions of $R_{J_n A_1}(t_a)$, $R_{J_n A_2}(t_a)$ and $R_{J_n A_3}(t_a)$ are respectively expressed as follows:

$$R_{J_n A_2}(t_a) = \sqrt{(x_n - vt_a)^2 + y_n^2 + (H - h_n)^2} = R_{J_n} - \frac{vx_n}{R_{J_n}} t_a + \frac{v^2}{2R_{J_n}} t_a^2 \quad (20)$$

$$R_{J_n A_1}(t_a) = \sqrt{(x_n - vt_a + D)^2 + y_n^2 + (H - h_n)^2} = R_{J_n A_2}(t_a) + \frac{x_n D - vDt_a + D^2}{R_{J_n}} \quad (21)$$

$$R_{J_n A_3}(t_a) = \sqrt{(x_n - vt_a - D)^2 + y_n^2 + (H - h_n)^2} = R_{J_n A_2}(t_a) - \frac{x_n D - vDt_a - D^2}{R_{J_n}} \quad (22)$$

where $R_{J_n} = \sqrt{x_n^2 + y_n^2 + (H - h_n)^2}$.

To generate the false moving target F , the intercepted signal is performed by phase modulation, time delay modulation and amplitude modulation. The baseband jamming signal of antenna A_1 and A_3 are respectively expressed as follows:

$$S_{F_1}(t_r, t_a) = \sum_{n=1}^N \left\{ G \rho_n a_r \left(t_r - \frac{R_{F_1}^n(t_a)}{c} \right) a_{az} \left(t_a - \frac{x'_m}{v} \right) \times \exp \left[-j \frac{2\pi}{\lambda} R_{F_1}^n(t_a) \right] \exp \left[j\pi \gamma \left(t_r - \frac{R_{F_1}^n(t_a)}{c} \right)^2 \right] \right. \\ \left. * \left[\delta \left(t_r - \frac{\Delta R_n(t_a)}{c} \right) \exp \left(-j \frac{2\pi}{\lambda} \Delta R_n(t_a) \right) \right] \right\} \quad (23)$$

$$S_{F_3}(t_r, t_a) = \sum_{n=1}^N \left\{ G \rho_n a_r \left(t_r - \frac{R_{F_3}^n(t_a)}{c} \right) a_{az} \left(t_a - \frac{x'_m}{v} \right) \times \exp \left[-j \frac{2\pi}{\lambda} R_{F_3}^n(t_a) \right] \exp \left[j\pi \gamma \left(t_r - \frac{R_{F_3}^n(t_a)}{c} \right)^2 \right] \right. \\ \left. * \left[\delta \left(t_r - \frac{\Delta R_n(t_a)}{c} \right) \exp \left(-j \frac{2\pi}{\lambda} \Delta R_n(t_a) \right) \right] \right\} \quad (24)$$

where G is jamming amplitude gain, $*$ denotes the convolution operation, and ρ_n is the jamming amplitude coefficients. $\Delta R_n(t_a)$ is denoted as the instantaneous slant range difference between the n th jammer and the moving target M , which can be shown as follows:

$$\Delta R_n(t_a) = 2 [R_{MA_2}(t_a) - R_{JA_2}(t_a)] \quad (25)$$

Then, after SAR imaging processing, the SAR images of false target F obtained based on (11) and (12) can be shown as follows:

$$I_{F_1} \left(t_r, t_a + \frac{D}{v} \right) = GI_M(t_r, t_a) \sum_{n=1}^N \rho_n A_n \quad (26)$$

$$I_{F_3}(t_r, t_a) = GI_M(t_r, t_a) \sum_{n=1}^N \rho_n B_n \quad (27)$$

where

$$A_n = \exp \left[\frac{j4\pi D}{\lambda R_{J_n}} \left(x'_m - \frac{x_n}{2} \right) \right] \quad (28)$$

$$B_n = \exp \left(\frac{j4\pi D x_n}{\lambda R_{J_n} 2} \right) \quad (29)$$

In order to generate a verisimilar false moving target, based on the DPCA technique, the detection result of the false moving target F should be equal to that of the moving target M by controlling variables G and ρ_n . It will be illustrated as follows:

$$\begin{aligned} I_{DPCA}^F(t_r, t_a) &= |I_{F_1}(t_r, t_a + D/v) - I_{F_3}(t_r, t_a)| \\ &= 2|I_M(t_r, t_a)| \cdot \left| \sin \left[\frac{2\pi D(x'_m - x_n)}{\lambda R_M} \right] \right| \\ &= I_{DPCA}^M(t_r, t_a) \end{aligned} \quad (30)$$

Based on the ATI technique, the interferometric phase of the false moving target F should be equal to that of the moving target M as follows:

$$\begin{aligned} \hat{\phi}_F &= \arg[I_{F_3}(t_r, t_a) \cdot I_{F_1}^*(t_r, t_a + D/v)] \\ &= \frac{4\pi D(x'_m - x_n)}{\lambda R_M} \\ &= \hat{\phi}_M \end{aligned} \quad (31)$$

Because the detection result and the interferometric phase of the false moving target F are equal to those of the moving target M , jammers will generate the verisimilar false moving target F that will be detected with DPCA technique and relocated in the desired positions with ATI technique.

Therefore, how to solve jamming amplitude coefficients ρ_n and jamming amplitude gain G becomes an important issue in this paper.

III. A MULTIPLE-JAMMER DECEPTIVE JAMMING METHOD BASED ON PARTICLE SWARM OPTIMIZATION

The proposed method contains three main parts. First, a novel jamming problem modeling idea is proposed based on an optimization problem. Second, the candidate variables ρ_n is calculated by PSO, and the best coefficients are selected from the candidate coefficients set based on the amplitude evaluation indicator. Finally, the implementation flowchart is presented.

A. JAMMING OPTIMIZATION PROBLEM PRDUCTION

The detection result of the false target F generated by multiple jammers consists of high order terms according to (26) and (27). It is reasonable to model the jamming result based on a polynomial function, where the jamming amplitude coefficients ρ_n represents the polynomial coefficients. Hence the jamming problem can be solved via estimating the polynomial coefficients ρ_n . The number of the jammers N is equal to the polynomial order, and the estimated polynomial coefficient vector can be reformed as $\hat{\mathbf{P}}_N = [\hat{\rho}_1 \hat{\rho}_2 \cdots \hat{\rho}_N]$.

Then, (26) and (27) can be respectively changed as follows:

$$\hat{I}_{F_1} \left(t_r, t_a + \frac{D}{v} \right) = G\hat{\mathbf{P}}_N \mathbf{A} \quad (32)$$

$$\hat{I}_{F_3}(t_r, t_a) = G\hat{\mathbf{P}}_N \mathbf{B} \quad (33)$$

$$\mathbf{A} = [A_1 \ A_2 \ \cdots \ A_n]^T \quad (34)$$

$$\mathbf{B} = [B_1 \ B_2 \ \cdots \ B_n]^T \quad (35)$$

where $\hat{\mathbf{P}}_N \in \mathbf{R}^N$, $\mathbf{A} \in \mathbf{R}^N$ and $\mathbf{B} \in \mathbf{R}^N$.

The jamming problem can be considered as an optimization problem as follows:

$$\min_{\rho \in \mathbf{R}^N} f(\hat{\mathbf{P}}_N) \quad (36)$$

where $f(\hat{\mathbf{P}}_N) = |\hat{\phi}_F - \hat{\phi}_M|$ is a particle fitness.

B. PSO-BASED POLYNOMIAL COEFFICIENTS SOLUTION METHOD

Compared with conventional optimization techniques like GAs and quasi-Newton algorithm, PSO is more of simplicity and robustness [26], [27]. Hence, a PSO-based global optimization method is used in this section. The estimated polynomial coefficient vector $\hat{\mathbf{P}}_N$ can be denoted by the particles. The procedure of PSO is presented in [28]. The update equations of each particle's position and velocity are described as follows:

$$\begin{aligned} \mathbf{v}_n^l &= \omega \mathbf{v}_n^{l-1} + c_1 r_1 (\mathbf{z}_n^{l-1, pbest} - \mathbf{z}_n^{l-1}) \\ &\quad + c_2 r_2 (\mathbf{z}_n^{l-1, gbest} - \mathbf{z}_n^{l-1}) \end{aligned} \quad (37)$$

$$\mathbf{z}_n^l = \mathbf{z}_n^{l-1} + \mathbf{v}_n^l \quad (38)$$

where n is the particle index, \mathbf{v} is individual velocity and \mathbf{z} is position. The total number of the particles is N and l is the iteration index that is strictly limited below the maximum l_{\max} . $c_1, c_2 > 0$ denote two positive accelerate constants. Generally, $r_1, r_2 \in \text{rand}(0, 1)$. $\mathbf{z}_n^{l-1, pbest}$ is the best solution that the n th particle has been found after $l-1$ iterations, while $\mathbf{z}^{l-1, gbest}$ is the best solution that the whole swarm has been found. ω is the inertia weight coefficient. According to (36), the smaller the cost function is, the better the corresponding particle is.

However, the smaller the cost function is, the more the computational burden is. Thus, the threshold of $f(\hat{\mathbf{P}}_N)$ is accepted as follows [18]:

$$f(\hat{\mathbf{P}}_N) \leq \frac{4\pi D P_a}{\lambda R_M 2} \quad (39)$$

where P_a is the azimuth resolution of the SAR images. Its advantage is that time used to obtain the candidate coefficient vectors is decreased. Moreover, the more times PSO is used, the more coefficient vectors can be acquired. Then, the lowest jamming amplitude coefficient vector can be selected from the candidate coefficient vectors sets.

The amplitude gain G makes the false target similar to the moving target in the detection result with DPCA technique.

G is related with $\hat{\mathbf{P}}_N$. According to (30), (32) and (33), G is expressed as follows:

$$G = \frac{I_{DPCA}^M(t_r, t_a)}{I_{DPCA}^F(t_r, t_a)} = \frac{I_{DPCA}^M(t_r, t_a)}{|\hat{\mathbf{P}}_N \mathbf{A} - \hat{\mathbf{P}}_N \mathbf{B}|} \quad (40)$$

Next, in order to choose the best solution that can lead to the lowest jamming energy, the amplitude evaluation indicator can be described by the means of $G\hat{\mathbf{P}}_N$ as follows:

$$\hat{\delta} = \frac{G}{N} \sum_{n=1}^N \hat{\rho}_n \quad (41)$$

Assume that the number of episodes is E which is related to the jamming decision-making time. Thus, during the process, there will be a sequence of the candidate variables G_E and vectors $\hat{\mathbf{P}}_N^E$. Then, the best variable G^* and vector $\hat{\mathbf{P}}_N^*$ can be chosen as follows:

$$\min_e \frac{G_e}{N} \sum_{n=1}^N \hat{\rho}_n^e \quad (42)$$

where e is the index of episode.

C. IMPLEMENTATION FLOWCHAR

An implementation flowchart of the proposed method is summarized as shown in Fig. 2.

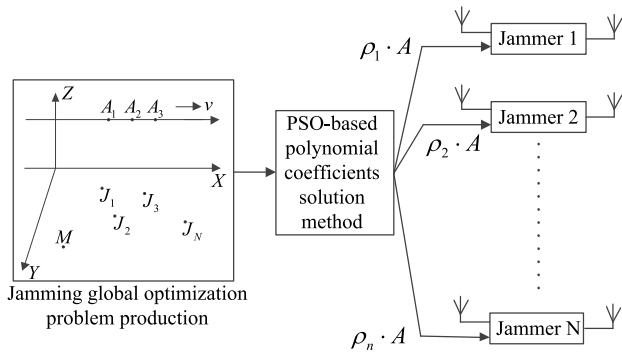


FIGURE 2. Implementation flowchart.

The process of the proposed method has the following three steps:

First, based on the jamming geometry, DPCA technique and ATI technique, an optimization problem is established by making interferometric phase of a moving target M and that of a false target F equal.

Second, the PSO-based method is implemented in loop to estimate the candidate amplitude gain G_L and polynomial jamming amplitude coefficient vector $\hat{\mathbf{P}}_N^L$. Then, the best variable G^* and vector $\hat{\mathbf{P}}_N^*$ will be chosen by using the amplitude evaluation indicator.

Finally, the best variable G^* and vector $\hat{\mathbf{P}}_N^*$ will be transmitted to each jammer. Then, the intercepted radar signal will be performed by time-delay modulation and amplitude modulation to generate jamming signal. The jamming signal

will be retransmitted to the radar, and then the false target will be detected in the desired azimuth position based on DPCA and ATI technique.

IV. EXPERIMENT RESULTS AND ANALYSIS

In this section, compared with the effect of the traditional method in [23], several simulated experiments are designed to verify the effectiveness of the proposed method. The azimuth and ground range length of the illuminated area are 200 m and 100 m, respectively. The Signal Noise Ratio (SNR) is assumed as 13.2 dB where detection probability is 0.9 and false-alarm probability is 10^{-6} [29]. The simulation parameters are shown in TABLE 1.

TABLE 1. Simulation parameters.

Symbol	Parameters	Value
v	SAR velocity	200 m/s
PRF	pulse repetition frequency	1170 Hz
D	effective baseline	2.77 m
H	altitude	5000 m
T_r	pulse duration	20 μ s
B_r	signal bandwidth	200 MHz
T_a	target exposure time	1.5 s
f_0	Radar center frequency	10 GHz
E	episode	30

A. A POINT TARGET SIMULATION

The real moving target is set in the illuminated area for contrast analysis. Its coordinate is (20020, 20, 0) with the azimuth velocity $v_x = 0.2$ m/s and the range velocity $v_y = 0.15$ m/s.

Assume that four jammers, $N = 4$, are used to generate the verisimilar false moving target, which is the same as the real moving target. The coordinates of four jammers J_1, J_2, J_3 , and J_4 are listed in TABLE 2. In addition, after 30 episodes with 100 iterations in each episode, the jamming amplitude coefficients and amplitude gain are also listed.

TABLE 2. Jammers parameters and according coefficients.

Jammers	Positions	Jamming Amplitude Coefficient	Amplitude Gain
J_1	(20000, 5000, 0) m	0.0053	
J_2	(20000, 5000, 37) m	0.4273	1.900
J_3	(20000, 5000, 74) m	0.6574	
J_4	(20000, 5000, 112) m	-1.6164	

The SAR imaging results of the real moving target and false moving target are shown in Fig. 3 and both of them are well imaged and focused in the SAR images. To evaluate the jamming effect, the correlation coefficient, which is the detailed jamming performance evaluation indicator, is calculated in this paper [13]. The correlation coefficient of the

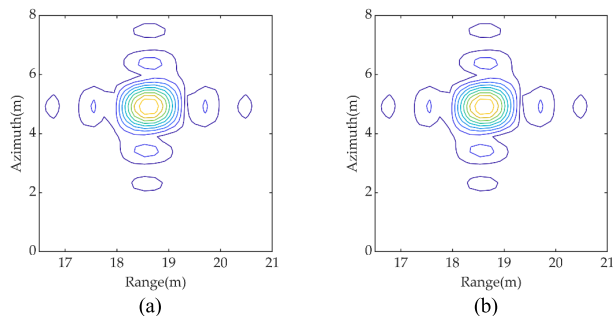


FIGURE 3. Contour plots. (a) The real moving target. (b) The false moving target.

jamming results is 0.9999 which is approximately equal to 1, that is to say, the false moving target are nearly the same as the real moving target.

Especially, the proposed method aims at generating moving targets against prescreening and detection before being focused and recognized. Thus, the defocused target is directly detected by suppressing the stationary target, and the detected targets will be further focused by estimating moving target parameters. If the false target is similar to the moving target, the computational burden of radar will be raised and making-decision will be misled. Focusing is not concerned in this paper, so the simulated targets are not very well focused. In addition, the defocused target will not cause difficulties in evaluating the effectiveness of the proposed method. The jamming signal and echo are processed as the same detection result by the same SAR processing, DPCA technique and ATI technique. That is to say, the proposed method will generate the same detection result, even the moving target is defocused.

The corresponding azimuth sectional plots are presented in Fig. 4 for contrast analysis.

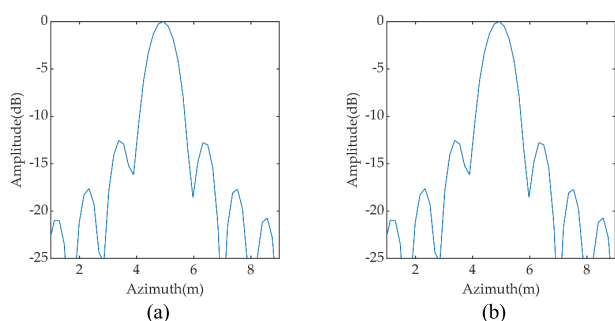


FIGURE 4. Azimuth sectional plots. (a) The real moving target. (b) The false moving target.

As seen from the figure, the real moving target and the false moving target are almost similar to each other. Detailed jamming evaluating indicators, including the range position, the azimuth position, the impulse response width (IRW), and the peak sidelobe ratio (PSLR) are calculated in TABLE 3 [1].

As shown in TABLE 3, the range position, the azimuth position and IRW are the same. Errors are obviously small, that is to say, the imaging result of the false target obtained has almost the same quality as that of the real target. So the

TABLE 3. SAR image quality parameters.

Indicators	Real moving target	False moving target	Error
Range position (m)	18.5349	18.5349	
Azimuth position (m)	4.9361	4.9361	
IRW (m)	0.9819	0.9819	1.900
PSLR (dB)	-12.55	-12.54	

proposed method is able to generate a false moving target with high fidelity against SAR.

After DPCA technique, the detection results are shown in Fig. 5. As seen in the figure, contour plots of the real moving targets and that of the false moving target look the same, and the correlation coefficient of the jamming results is 0.9987, which means the detection results of the false target are the same as those of the real moving target.

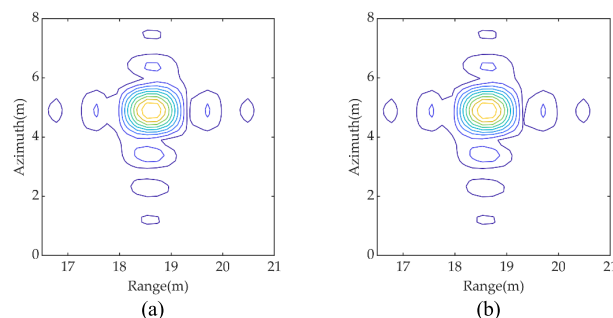


FIGURE 5. Contour plots. (a) The real moving target. (b) The false moving target.

For further comparison analysis, the azimuth sectional plots are presented in Fig. 6. In addition, the corresponding evaluating indicators are listed in TABLE 4.

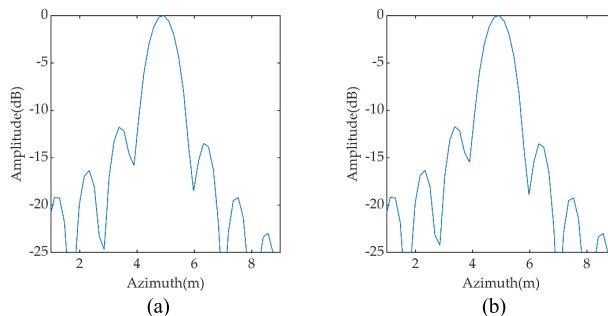


FIGURE 6. Azimuth sectional plots. (a) The real moving target. (b) The false moving target.

TABLE 4. Detection results of image quality parameters.

Indicators	Real moving target	False moving target	Error
Range position (m)	18.5349	18.5349	0
Azimuth position (m)	4.9361	4.9361	0
IRW (m)	0.9401	0.9364	0.037
PSLR (dB)	-11.76	-11.72	-0.04

As presented in TABLE 4, the range position and the azimuth position are the same. The IRWs and PSLRs of the real targets and the false targets are also almost the same with

only several hundredths of a decibel difference. Therefore, the proposed method is able to generate false moving target with high fidelity in the detection results based on DPCA technology.

When the moving target is detected, its moving parameters, interferophase, initial azimuth position, and the ground range velocity, are also estimated based on ATI technology. Radar will use the initial azimuth position to relocate the targets. The estimations of target velocity and initial azimuth position are listed in TABLE 5.

TABLE 5. Estimations of target velocity and initial azimuth positions.

Index	Interferophase (rad)	Initial azimuth position (m)	Velocity (m/s)
The real moving target	0.8476	15.0568	-0.1460
The false moving target	0.8501	15.1015	-0.1460
Error	-0.005	-0.0447	0

The interferophase of the real targets and the false targets are also nearly the same with only several hundredths of a decibel difference. Then, the low error interferophase will lead to the low error of initial azimuth position, which is obviously small. In addition, the velocities of the real moving targets and the false moving targets are the same.

In other words, SAR imaging result, the detection result and moving parameters of the false moving targets obtained can have almost the same quality as those of the real moving target. Therefore, the proposed method is able to generate false targets based on ATI technology.

B. COMPARING THE PROPOSED METHOD AND THE TRADITIONAL METHOD

Assume that two jammers, J_1 and J_4 , are used by the traditional method in [23] to generate a verisimilar false moving target which simulates a real moving target. In addition, two jammers, J_2 and J_3 , are added with the proposed method to generate a false moving target which simulates the same real moving target for contrast analysis. Then, the coordinates and variables of the jammers are shown in TABLE 6.

In TABLE 7, the false target 1 is generated with the proposed method, and the false target 2 is generated with the traditional method. Meanwhile, the estimations of the target velocity and initial azimuth position are also shown in the table. Interferophase, initial azimuth position, and the ground

TABLE 6. Jammers parameters and according coefficients.

Jammers	Positions	Coefficients of the traditional method	Coefficients of the proposed method
J_1	(20000, 5000, 0) m	-44.73-15.80j	0.0106
J_2	(20000, 5000, 37) m	-	0.8546
J_3	(20000, 5000, 74) m	-	1.3148
J_4	(20000, 5000, 112) m	-45.58-15.81j	-3.2328

TABLE 7. Estimations of target velocity and initial azimuth positions.

Index	Interferophase (rad)	Initial azimuth position (m)	Velocity (m/s)
The real moving target	0.8476	15.0568	-0.1460
The false target 1	0.8501	15.1015	-0.1460
The false target 2	0.8522	15.1392	-0.1460

range velocity, are nearly the same. Thus, both the proposed method and the traditional method are able to generate the verisimilar false moving target.

However, according to the coefficients shown in TABLE 7, when the distance between J_1 and J_4 required by the traditional jamming method is not satisfied, the jamming power is higher than that required by the proposed method. The less jamming power is, the easier realization is. Therefore, the proposed jamming method is able to generate verisimilar false moving targets with low power and easy realization.

V. CONCLUSION

It is difficult to estimate jamming coefficients using mathematical analysis which makes the processing of solution too complex and trivial, such as monotonicity. Moreover, coefficients estimated by solving equation that are constructed by making interferometric phase of a false target and a moving target be equal will lead to obtain a unique solution of jamming coefficients with a constraint of distance between jammers. To remove the distance limitation, compared with previous works, the contribution of this paper is that a novel jamming problem modeling idea is proposed based on an optimization problem. Therefore, a PSO-based method is proposed to estimate the coefficients. When the distance between jammers required by the traditional jamming method is not satisfied, the jamming power required by the proposed method is lower than that required by traditional methods. By using the jamming evaluating indicators, including the range position, the azimuth position, IRW, PSLR, and correlation coefficient, the proposed method is able to generate the verisimilar false moving target. Furthermore, the proposed method introduces a novel jamming coefficient acquirement structure, which could be suitable for this problem in the field of ECM. Although the PSO-based method could introduce a heavy computational burden, device capabilities could be improved to meet this challenge, and the improved method based on paralleled PSO algorithm is expected to reduce parameter acquisition time in the future.

REFERENCES

- [1] I. G. Cumming and F. H. Wong, *Digital Processing of Synthetic Aperture Radar Data: Algorithms and Implementation*. Norwood, MA, USA: Artech House, 2005.
- [2] D. Cerutti-Maori, I. Sikaneta, and C. H. Gierull, "Optimum SAR/GMTI processing and its application to the radar satellite RADARSAT-2 for traffic monitoring," *IEEE Trans. Geosci. Remote Sens.*, vol. 50, no. 10, pp. 3868–3881, Oct. 2012.
- [3] C. H. Gierull, I. Sikaneta, and D. Cerutti-Maori, "Two-step detector for RADARSAT-2's experimental GMTI mode," *IEEE Trans. Geosci. Remote Sens.*, vol. 51, no. 1, pp. 436–454, Jan. 2013.

- [4] G. Lv, Y. Li, G. Wang, and Y. Zhang, "Ground moving target indication in SAR images with symmetric Doppler views," *IEEE Trans. Geosci. Remote Sens.*, vol. 54, no. 1, pp. 533–543, Jan. 2016.
- [5] T. Liu, W. Li, and J. Guan, "Deep learning based object detection in optical remote sensing images: A survey," *Radio Commun. Technol.*, vol. 46, no. 6, pp. 624–634, Jan. 2020.
- [6] S. Chiu and C. Livingstone, "A comparison of displaced phase centre antenna and along-track interferometry techniques for RADARSAT-2 ground moving target indication," *Can. J. Remote Sens.*, vol. 31, no. 1, pp. 37–51, 2005.
- [7] D. Cerutti-Maori and I. Sikaneta, "A generalization of DPCA processing for multichannel SAR/GMTI radars," *IEEE Trans. Geosci. Remote Sens.*, vol. 51, no. 1, pp. 560–572, Jan. 2013.
- [8] S. Tanelli, S. L. Durden, and M. P. Johnson, "Airborne demonstration of DPCA for velocity measurements of distributed targets," *IEEE Geosci. Remote Sens. Lett.*, vol. 13, no. 10, pp. 1415–1419, Oct. 2016.
- [9] B. Zhao, F. Zhou, and Z. Bao, "Deception jamming for squint SAR based on multiple receivers," *IEEE J. Sel. Topics Appl. Earth Observ. Remote Sens.*, vol. 8, no. 8, pp. 3988–3998, Aug. 2015.
- [10] X. Wu, X. Wang, and J. Liang, "Modulation jamming method for high-vivid false uniformly-moving targets against SAR-GMTI," *J. Astron.*, vol. 33, no. 10, pp. 1472–1479, 2012.
- [11] F. Zhou, B. Zhao, M. Tao, X. Bai, B. Chen, and G. Sun, "A large scene deception jamming method for space-borne SAR," *IEEE Trans. Geosci. Remote Sens.*, vol. 51, no. 8, pp. 4486–4495, Aug. 2014.
- [12] L. Huang, C. Dong, Z. Shen, and G. Zhao, "The influence of rebound jamming on SAR GMTI," *IEEE Geosci. Remote Sens. Lett.*, vol. 12, no. 2, pp. 399–403, Feb. 2015.
- [13] X.-R. Shi, F. Zhou, B. Zhao, M.-L. Tao, and Z.-J. Zhang, "Deception jamming method based on micro-Doppler effect for vehicle target," *IET Radar, Sonar Navigat.*, vol. 10, no. 6, pp. 1071–1079, Jul. 2016.
- [14] B. Zhao, L. Huang, F. Zhou, and J. Zhang, "Performance improvement of deception jamming against SAR based on minimum condition number," *IEEE J. Sel. Topics Appl. Earth Observ. Remote Sens.*, vol. 10, no. 3, pp. 1039–1055, Mar. 2017.
- [15] Q. Sun, T. Shu, K.-B. Yu, and W. Yu, "Efficient deceptive jamming method of static and moving targets against SAR," *IEEE Sensors J.*, vol. 18, no. 9, pp. 3610–3618, May 2018.
- [16] Q. Sun, T. Shu, B. Tang, and W. Yu, "Target deception jamming method against spaceborne synthetic aperture radar using electromagnetic scattering," *J. Appl. Remote Sens.*, vol. 12, no. 1, p. 1, Mar. 2018.
- [17] X. Chang, C. Dong, Z. Tang, and Y. Dong, "Mosaic scene deception jamming based on 2D separation modulation against SAR," *IET Radar, Sonar Navigat.*, vol. 13, no. 2, pp. 310–315, Feb. 2019.
- [18] X. Chang and C. Dong, "A barrage noise jamming method based on double jammers against three channel SAR GMTI," *IEEE Access*, vol. 7, pp. 18755–18763, 2019.
- [19] J. Zhang, D. Dai, Z. Qi, Y. Zeng, and S. Xiao, "Analysis of deceptive moving target generated by single jammer in multi-channel SAR-GMTI," in *Proc. Int. Appl. Comput. Electromagn. Soc. Symp. (ACES)*, Suzhou, China, Aug. 2017, pp. 1–2.
- [20] C. Dong and X. Chang, "A novel scattered wave deception jamming against three channel SAR GMTI," *IEEE Access*, vol. 6, pp. 53882–53889, 2018.
- [21] J. Zhang, S. Xing, D. Dai, Y. Li, and S. Xiao, "Three-dimensional deceptive scene generation against single-pass InSAR based on coherent transponders," *IET Radar, Sonar Navigat.*, vol. 10, no. 3, pp. 477–487, Mar. 2016.
- [22] J. Zhang, "Study on distributed cooperative jamming techniques against multichannel SAR," Ph.D. dissertation, Dept. Inf. Comput. Eng., Natl. Univ. Def. Technol., Changsha, Hunan, China, 2016.
- [23] Q. Sun, T. Shu, K.-B. Yu, and W. Yu, "A novel deceptive jamming method against two-channel SAR-GMTI based on two jammers," *IEEE Sensors J.*, vol. 19, no. 14, pp. 5600–5610, Jul. 2019.
- [24] X. Chang, Ch. Dong, Z. Tang, Y. Dong, and M. Liu, "False moving scene jamming method based on double jammers and magnitude modulation against SAR-GMTI," *J. Electron. Inf. Technol.*, vol. 40, no. 9, pp. 2190–2197, Sep. 2018.
- [25] X. Chang, Y. Li, and Y. Zhao, "An improved scattered wave deceptive jamming method based on a moving jammer beam footprint against a three-channel short-time SAR GMTI," *IEEE Sensors J.*, vol. 21, no. 4, pp. 4488–4499, Feb. 2021.
- [26] J. Nocedal and S. J. Wright, *Numerical Optimization*. New York, NY, USA: Springer, 2006.
- [27] J. Kennedy and R. C. Eberhart, *Swarm Intelligence*. San Diego, CA, USA: Academic, 2001.
- [28] L. Liu, F. Zhou, M. Tao, P. Sun, and Z. Zhang, "Adaptive translational motion compensation method for ISAR imaging under low SNR based on particle swarm optimization," *IEEE J. Sel. Topics Appl. Earth Observ. Remote Sens.*, vol. 8, no. 11, pp. 5146–5157, Nov. 2015.
- [29] D. K. Barton, *Radar System Analysis and Modeling*. Norwood, MA, USA: Artech House, 2005.



XIN CHANG was born in Shijiazhuang, Hebei, China, in 1990. He received the B.S. degree in electrical engineering from Handan University, Handan, China, in 2014, and the M.Eng. degree in electronics and communication engineering and the Ph.D. degree in electronics science and technology from the School of Electronic Engineering, Xidian University, Xi'an, China, in 2017 and 2020, respectively. He currently holds the postdoctoral position with The 54th Research Institute of China Electronics Technology Group Corporation (CETC54), Shijiazhuang, and Xidian University. His main research interests include electronic countermeasure (ECM), electronic warfare system simulation, and cognitive electronic warfare.



YANBIN LI was born in Shijiazhuang, Hebei, China, in 1966. He received the B.S. degree from Tianjin University, Tianjin, China, in 1985, the M.E. degree from The 54th Research Institute of China Electronic Technology Group Corporation (CETC54), Shijiazhuang, in 1988, and the Ph.D. degree from Shanghai Jiaotong University, Shanghai, China, in 1995. He is currently a Chief Expert with China Electronic Technology Group Corporation and a Chief Scientist with The 54th Research Institute of China Electronics Technology Group Corporation (CETC54). His main research interests include electronic countermeasure (ECM) and cognitive electronic warfare.



YAN ZHAO was born in Gansu, China, in 1981. He received the B.S. degree from the School of Telecommunications Engineering, Xidian University, Xi'an, China, in 2003, and the M.S. degree from the School of Electronic Engineering, Xidian University, in 2009, where he is currently pursuing the Ph.D. degree with the National Laboratory of Radar Signal Processing. He is currently with The 54th Research Institute of China Electronics Technology Group Corporation (CETC54), Shijiazhuang, China. His main research interests include array signal processing and radar signal processing.



YUFENG DU was born in Shanxi, China, in 1981. He received the bachelor's degree in electrical engineering and automation and the master's degree in electronic and communication engineering from Xidian University, in July 2003 and December 2012, respectively. He is currently a Deputy Director with Hebei Key Laboratory of Electromagnetic Spectrum Cognition and Control, The 54th Research Institute of China Electronics Technology Group Corporation (CETC54), Shijiazhuang, China.

...